

# Apparent Dispersion in Transient Groundwater Flow

DANIEL J. GOODE AND LEONARD F. KONIKOW

U.S. Geological Survey, Reston, Virginia

This paper investigates the effects of large-scale temporal velocity fluctuations, particularly changes in the direction of flow, on solute spreading in a two-dimensional aquifer. Relations for apparent longitudinal and transverse dispersivity are developed through an analytical solution for dispersion in a fluctuating, quasi-steady uniform flow field, in which storativity is zero. For transient flow, spatial moments are evaluated from numerical solutions. Ignored or unknown transients in the direction of flow primarily act to increase the apparent transverse dispersivity because the longitudinal dispersivity is acting in a direction that is not the assumed flow direction. This increase is a function of the angle between the transient flow vector and the assumed steady state flow direction and the ratio of transverse to longitudinal dispersivity. The maximum effect on transverse dispersivity occurs if storativity is assumed to be zero, such that the flow field responds instantly to boundary condition changes.

## INTRODUCTION

Large-scale dispersion of solutes in groundwater (macrodispersion) is now generally believed to result from spatial variations in the velocity field caused by spatial variability in aquifer properties (primarily hydraulic conductivity). However, groundwater velocity is also a function of the hydraulic gradient, which can change over time because of changes in the relative magnitudes and locations of hydraulic stresses imposed on an aquifer system. Thus as the spatial distribution of recharge, well withdrawals, and (or) surface water stage, for example, vary with time, a temporal variability in the magnitude and direction of velocity will occur. For example, in a study of a site where hydrocarbons leaked to the water table, *LaFave* [1989] found that the groundwater flow direction changed approximately 90 degrees in less than 4 months in response to changing flow conditions in a nearby intermittent stream.

Aquifer heterogeneity contributes to plume spreading because it generates variability in the fluid velocity, causing different parts of the plume to move at different rates. Temporal fluctuations in recharge, discharge, or boundary conditions will also increase velocity variance and thus might also be expected to contribute to plume spreading. Just as ignorance of aquifer heterogeneity (and spatially variable advection) is compensated for by using a higher than local dispersivity value in a classical solute transport analysis, so could ignoring or neglecting the true transient nature of a flow system yield compensating changes in assumed dispersivity values.

### Previous Research

Many (if not most) analyses of field-scale solute transport problems assume that an average or steady state groundwater flow field prevails. In these cases the effects of flow field transients are usually considered to be negligible or of second-order importance. *Sykes et al.* [1982, p. 1699] used a steady state flow model in their analysis of contaminant migration from a landfill. However, they concluded that "... much of the [horizontal] lateral dispersion [is] caused

This paper is not subject to U.S. copyright. Published in 1990 by the American Geophysical Union.

Paper number 90WR01420.

by a changing potentiometric surface rather than 'tortuosity' " because of consequent changes in both magnitude and orientation of velocity vectors. On the other hand, *Duguid and Reeves* [1977], in applying a two-dimensional transport model to a site at the Oak Ridge National Laboratory, found no substantial difference between using average and transient rainfall boundary conditions. Although they found variations in concentration attributable to the transient rainfall to be negligible, it should be noted that this recharge was uniform over the surface area, so temporal changes in the spatially uniform rate would not induce significant changes in the direction of flow. The results of both of these studies are consistent with those of *Wierenga* [1977], who showed that, for one-dimensional transport using constant dispersivity, fluctuations in velocity magnitude alone did not significantly affect longitudinal dispersion.

*Kinzelbach and Ackerer* [1986] (see also *Ackerer and Kinzelbach* [1985]) present expressions for apparent longitudinal and transverse dispersivities,  $\alpha_{La}$  and  $\alpha_{Ta}[L]$ , in transient flow:

$$\alpha_{La} = \alpha_L \frac{\overline{V_L^2}}{\overline{VV}} + \alpha_T \frac{\overline{V_T^2}}{\overline{VV}} \quad (1)$$

$$\alpha_{Ta} = \alpha_T \frac{\overline{V_L^2}}{\overline{VV}} + \alpha_L \frac{\overline{V_T^2}}{\overline{VV}}$$

where  $\alpha_L$  and  $\alpha_T$  are the true longitudinal and transverse dispersivities [L], respectively,  $V_L$  is the component of velocity in the mean (longitudinal) flow direction [ $LT^{-1}$ ], and  $V_T$  is the component of velocity transverse to the mean flow direction [ $LT^{-1}$ ]. The overbars in (1) indicate the time average. *Kinzelbach and Ackerer* [1986] also report that for the case of temporal variability in the direction of flow only, with the magnitude of velocity constant in time, the sum of the apparent dispersivities given by (1) is equal to the sum of the true dispersivities:

$$\alpha_{La} + \alpha_{Ta} = \alpha_L + \alpha_T \quad (2)$$

*Kinzelbach and Ackerer* [1986] fit an observed plume using two models. One model assumed transient flow in response to seasonal fluctuations and used dispersivities  $\alpha_L = 81.3$  m,

and  $\alpha_T = 0.7$  m. The other model assumed steady flow and used dispersivities  $\alpha_{La} = 80$  m, and  $\alpha_{Ta} = 2$  m. Assuming steady state flow, a suitable fit was obtained by increasing the transverse dispersion coefficient.

*Rehfeldt* [1988] applied the stochastic small-perturbation approach of *Gelhar and Axness* [1983] to investigate solute transport impacts of temporal variability in the hydraulic gradient. Both longitudinal and transverse dispersivity were increased by fluctuations in the direction and magnitude of velocity, although the effect on longitudinal dispersivity was generally insignificant.

Recently, *Naff et al.* [1989] postulated that small-scale velocity transients may be responsible for large transverse spreading observed at two intensively studied field sites. They show that adding time-dependent deterministic harmonics to the velocity, which change the flow direction, can result in significant increases in the variance of concentration in the transverse direction. They did not formulate the velocity fluctuations in terms of solutions to the flow equation. Rather, the temporal velocity variability was directly specified and considered independent of spatial velocity fluctuations.

#### Scope

The purpose of this study is to investigate the effects of temporal velocity fluctuations on apparent or calibrated dispersivities and to demonstrate under what, if any, conditions transverse spreading of a plume is significantly enhanced by transient changes in flow. The study focuses on changes in flow direction over time, rather than temporal changes in magnitude of velocity, because fluctuations in magnitude are unlikely to have a significant effect on dispersion.

Our approach is to compare transport in transient flow fields with that in steady state flow fields having equivalent average fluxes and flow directions. In deriving general relations between apparent dispersivity and parameters characterizing transient flow, we assume aquifer properties to be uniform to isolate the effects of temporal velocity fluctuations from those of aquifer heterogeneity. This approach allows us to derive explicit relations between certain parameters and apparent dispersivities, instead of being limited to expressions containing, for example, unknown time-average velocities. Further, consideration of uniform flow cases allows determination of uniform apparent dispersivities for the entire domain. We independently derive apparent dispersivity expressions similar to *Kinzelbach and Ackerer's* [1986] result, equation (1), through a convolution solution of the transport equation for the special case of quasi-steady (zero storativity) uniform flow. However, we show that (2) does not hold for our case, and we argue that it does not hold in general.

Our analysis is similar to the moments analysis of *Naff et al.* [1989] in that we consider deterministic changes in the velocity. However, our velocity changes are induced by solving the flow equation with temporally variable boundary conditions. This leads to both temporal and spatial velocity fluctuations that are physically consistent.

#### GOVERNING EQUATIONS AND NUMERICAL SOLUTION

A transient, two-dimensional, areal, groundwater flow equation can be written [*Bear*, 1979]:

$$S \frac{\partial h}{\partial t} = \frac{\partial}{\partial x_i} \left( T_{ij} \frac{\partial h}{\partial x_j} \right) - W \quad (3)$$

where  $S$  is the aquifer storativity or storage coefficient [dimensionless],  $h$  is potentiometric head [L],  $t$  is time [T],  $x_i$  are the horizontal spatial coordinates ( $x_1 = x$  and  $x_2 = y$ ) [L],  $T_{ij}$  is the transmissivity tensor [ $L^2 T^{-1}$ ], and  $W$  is the volumetric discharge (+) or recharge (-) rate per unit area [ $L T^{-1}$ ]. In this study we assume that  $T$  is constant, uniform, and isotropic.  $S$  is also constant and uniform, and  $W$  is nonzero only at a source of solute mass, although the magnitude of  $W$  is so small that it is insignificant for the flow problem. For transient flow the initial head is specified at all locations. Possible boundary conditions for (3) include specified head and specified flux. Under quasi-steady conditions ( $S = 0$ ) the flow system responds instantly to changes in boundary and recharge/discharge conditions.

A conventional form of the advection-dispersion equation governing nonreactive solute transport in two dimensions is [after *Konikow and Grove*, 1977]:

$$\epsilon b \frac{\partial C}{\partial t} = \frac{\partial}{\partial x_i} \left( \epsilon b D_{ij} \frac{\partial C}{\partial x_j} \right) - \epsilon b V_i \frac{\partial C}{\partial x_i} + W(C - C') \quad (4)$$

where  $C$  is the volumetric concentration of the solute [ $ML^{-3}$ ],  $\epsilon$  is porosity [ $L^3 L^{-3}$ ],  $b$  is the saturated thickness [L],  $D_{ij}$  is the dispersion tensor [ $L^2 T^{-1}$ ],  $V_i$  is the fluid seepage velocity vector [ $L T^{-1}$ ], and  $C'$  is the concentration in the source fluid ( $W < 0$ ) [ $ML^{-3}$ ]. For hydraulic sinks ( $W > 0$ ),  $C' = C$ .

If changes in concentration are small enough that they do not affect fluid properties, then the flow and transport equations are linked only by the velocity term and the fluid storage term ( $\epsilon b$ ). During transient flow the fluid storage term ( $\epsilon b$ ) changes because of changes in head and will be spatially variable. For the present work the initial value of ( $\epsilon b$ ) is uniform in space, and it is additionally constant in time for the steady and quasi-steady flow cases. Velocity can be determined from the solution of the flow equation (3) through Darcy's law and the relation of velocity to flux:

$$\epsilon b V_i = -T \frac{\partial h}{\partial x_i} \quad (5)$$

Conceptually, we assume that the scale of the transport problem is large relative to the correlation scale of hydraulic conductivity and that macrodispersion due to aquifer heterogeneity has reached a large-scale Fickian asymptote [*Gelhar and Axness*, 1983; *Dagan*, 1984]. We follow the conventions of neglecting molecular diffusion as a separate process and characterizing dispersion by the longitudinal and transverse dispersivities [e.g., *Bear*, 1979]:

$$D_{ij} = \alpha_T |V| \delta_{ij} + (\alpha_L - \alpha_T) \frac{V_i V_j}{|V|} \quad (6)$$

where  $\delta_{ij} = 1$  for  $i = j$ , and  $\delta_{ij} = 0$  otherwise, and  $|V|$  is the magnitude of velocity:

$$|V| = [(V_x)^2 + (V_y)^2]^{1/2} \quad (7)$$

To solve these governing equations in the example simulations, we apply the numerical model of *Konikow and*

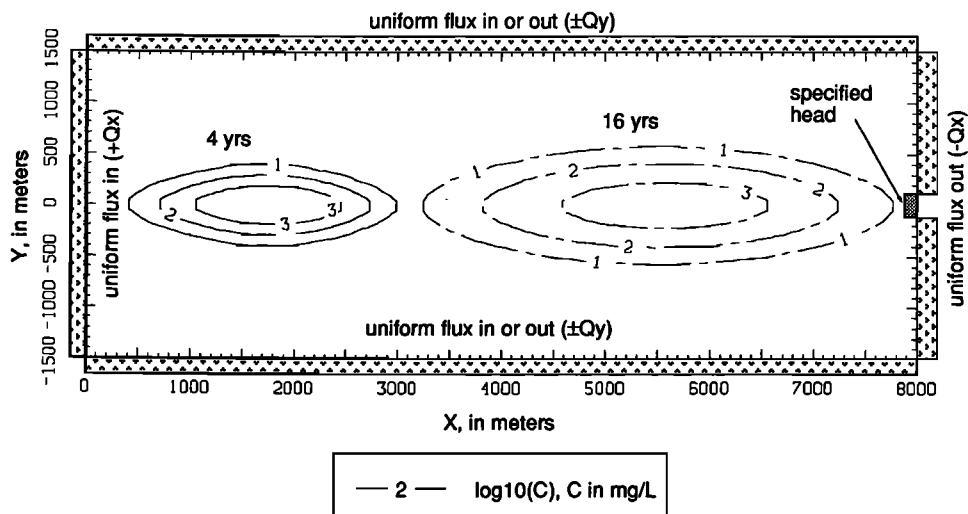


Fig. 1. Solute dispersion in steady state flow field for  $\alpha_L = 40$  m and  $\alpha_T = 2$  m. Also shown are model grid and boundary condition locations. The small tic marks represent the block size; the grid is 80 by 30 blocks.

Bredehoeft [1978]. In the numerical model the flow equation (3) is solved using implicit finite difference techniques. The transport equation (4) is solved using explicit finite difference techniques for dispersion, accumulation, and source terms and using the method-of-characteristics with moving particles for advection [Konikow and Bredehoeft, 1978; Goode and Konikow, 1989]. One advantage of this particular model is its ability to generate solutions to problems having zero or low dispersivity (large Peclet number) that exhibit minimal numerical dispersion or oscillation. Of course, the results presented would be essentially the same for any two-dimensional flow and transport simulator used with adequate discretization.

Aquifer properties are assumed to be uniform and hydraulic boundary conditions are changed over time to induce temporal variability in potentiometric heads and velocities. If we consider an aquifer having a rectangular domain (Figure 1), uniform flow in the  $x$  direction (from left to right) results from imposing constant flux per unit length of boundary into the aquifer on the left end of the domain ( $+Q_x$ , [ $L^2T^{-1}$ ]), constant flux out on the right end equal to the upstream flux ( $-Q_x$ ), and no-flow boundaries ( $Q_y = 0$ ) along the top and bottom. Head can be specified at the midpoint of the right boundary to provide a model head datum. Under these basic boundary conditions the flow direction will rotate if additional transient flux boundary conditions are applied along the top and bottom boundaries.

The effects of hydraulic transients on dispersive transport can be analyzed by comparison to the case of steady flow, where solute spreading is caused entirely by spatial heterogeneity. Figure 1 shows a numerical solution for advection and dispersion of solute mass in a uniform, steady state flow field having flow from left to right in the  $x$  direction. The solute, initially occupying a square area (four grid blocks at  $C_0 = 50,000$  mg/L), disperses more in the direction of flow than it does perpendicular (or transverse) to flow because the longitudinal dispersivity is 40 m, whereas the transverse dispersivity is only 2 m. The contours represent lines of equal concentration, the labels are  $\log_{10}(C)$  (so a value of 3, for example, indicates  $C = 1000$  mg/L), and the solute distribution is shown at 4 and 16 years. Figure 1 also shows

the location and types of numerical model boundary conditions, and the small tics on the axes indicate the block-centered, finite difference grid spacing. For the plume shown,  $Q_y = 0$ . The following model parameters are used for this and the following numerical examples:  $T = 0.001$  m<sup>2</sup>/s,  $b = 100$  m,  $\epsilon = 0.1$ , and the grid spacing is 100 m in both  $x$  and  $y$ . The flux boundary condition (volumetric flux per unit width) on the inflow boundary on the left is  $Q_x = 10^{-4}$  m<sup>2</sup>/s, and an identical flux out is applied on the right outflow boundary. The parameters used here result in velocity in the  $x$  direction of slightly less than 1 m/d. The width of the rectangular model area is specified sufficiently large so that the simulated plumes will not be affected significantly by the lateral boundaries of the domain.

To induce transient flow having mean flow in the  $x$  direction, mirror image boundary condition changes are applied along the top and bottom boundaries. During the first time period ( $0 < t < t_1$ ), constant flux out ( $-Q_y$ ) is specified along the top boundary and an equal constant flux in ( $+Q_y$ ) is specified along the bottom boundary. If equilibrium is established, steady state uniform flow is at an angle  $\theta = \tan^{-1}(Q_y/Q_x)$  to the  $x$  axis. During the second and third time periods the pattern is reversed, applying inward flux along the top boundary and outward flux along the bottom boundary. In this case, steady state flow is at an angle  $-\theta$ . Subsequently, the top and bottom boundary conditions are reversed after every two time periods. This pattern induces  $y$  velocity fluctuations, while the  $x$  velocity is unchanged from the steady state case. Thus the solute's center of mass moves alternatively in the positive and negative  $y$  directions within the modeled area. After every two time periods ( $t = (2n)t_1$ ), the center of mass returns to the centerline of the modeled area, and the time-averaged  $y$  velocity is zero.

#### APPARENT DISPERSIVITIES IN QUASI-STEADY UNIFORM FLOW

If plumes are simulated using a model assuming steady state flow, the calibrated dispersion parameters will account for the spreading due to pore-scale mixing, aquifer heterogeneity, and transient flow. For this work the apparent

longitudinal and transverse dispersivities are defined as those values that yield the best match or calibration of the solute transport model under steady state flow conditions to a plume that developed under transient-flow conditions. Thus the apparent dispersivities are functions of both the physical dispersion at the model scale, characterized by the true dispersivities as well as hydraulic transients in the aquifer. We use numerical experiments to quantify solute dispersion in transient-flow fields because analytical solutions are not available, and we characterize solute spreading using the method of moments. However, we can develop an analytical solution for the special case of quasi-steady flow ( $S = 0$ ), in which the flow field responds instantly to changing boundary conditions. The relations between apparent dispersivities and true dispersivities can be determined by comparing this quasi-steady solution to an analytical solution for transport in a steady state flow field that has a velocity corresponding to the mean velocity of the quasi-steady state case.

*Convolution Solution for Apparent Dispersivities*

An analytical solution for transport and dispersion of a Dirac pulse of unit solute mass in a quasi-steady uniform flow field can be obtained using convolution. For a frame of reference it is assumed that the mass is initially at the point ( $x = 0, y = 0$ ) and that flow is initially at an angle  $\theta$  to the  $x$  axis. After some time,  $t_1$ , the flow field changes direction to  $-\theta$ . The angle between the velocity vectors of the first and second time periods is  $2\theta$ . The angle of deviation of the flow field and the ratio of velocity components are related by

$$\sin \theta = V_T/V \quad \cos \theta = V_L/V \quad (8)$$

The solute distribution during the second time period is the convolution of the distribution at the end of the first period (the initial condition for the second period) times the instantaneous solution for a Dirac pulse. When the length of the second time period equals the length of the first time period ( $t = 2t_1; t - t_1 = t_1$ ), the center of mass has returned to the  $x$  axis, and the convolution equation reduces to (see the appendix)

$$C(x, y, t) = \frac{1}{\epsilon b} (4\pi Vt)^{-1} [(\alpha_L \cos^2 \theta + \alpha_T \sin^2 \theta) \cdot (\alpha_T \cos^2 \theta + \alpha_L \sin^2 \theta)]^{-1/2} \cdot \exp \left[ -\frac{(x - Vt \cos \theta)^2}{4(\alpha_L \cos^2 \theta + \alpha_T \sin^2 \theta)Vt} - \frac{y^2}{4(\alpha_T \cos^2 \theta + \alpha_L \sin^2 \theta)Vt} \right] \quad (9)$$

This can be compared to the analytical solution for the case of uniform steady state flow in the  $x$  direction [e.g., Bear, 1979] and is equivalent if the apparent velocity ( $V_a$ ) and apparent dispersivities are defined:

$$C(x, y, t) = \frac{1}{\epsilon b} (4\pi V_a t)^{-1} (\alpha_{La} \alpha_{Ta})^{-1/2}$$

$$\cdot \exp \left[ -\frac{(x - V_a t)^2}{4\alpha_{La} V_a t} - \frac{y^2}{4\alpha_{Ta} V_a t} \right] \quad (10)$$

where

$$V_a = V \cos \theta \quad (11)$$

$$\alpha_{La} = \alpha_L \cos \theta + \alpha_T \sin \theta \tan \theta \quad (12)$$

$$\alpha_{Ta} = \alpha_T \cos \theta + \alpha_L \sin \theta \tan \theta \quad (13)$$

As long as the time periods have the same length, and the angle of flow is the same ( $\theta$  or  $-\theta$ ), the relations in (11)–(13) are valid, and (10) yields the solute distribution at  $t = 2t_1, 4t_1, 6t_1, \dots, (2n)t_1$ .

This definition of apparent velocity (11) is equal to the time-averaged velocity at these times and does not include a contribution from the transverse velocity component. That is, the apparent velocity is equal to the longitudinal velocity  $V_a = V_L$ . The time-averaged transverse velocity at these times is zero. As shown by (9) and (10), using this  $V_a$  yields the appropriate translation of the plume in the  $x$  or mean longitudinal direction.

These apparent dispersivities can be derived for this special case using the expressions of Kinzelbach and Ackerer [1986]. However, those authors appear to have assumed that the magnitude of time-averaged velocity  $\bar{V}$  is equal to the actual velocity  $V$ . This assumption is necessary in order to derive their equality between the sum of the apparent dispersivities and the sum of the true dispersivities, equation (2) above. From our results, equations (12) and (13), the apparent dispersion coefficients are related to the true dispersion coefficients by

$$D_{La} + D_{Ta} = D_L + D_T \quad (14)$$

In contrast to the relation proposed by Kinzelbach and Ackerer [1986], equation (2) above, we find that the sum of the apparent dispersivities is larger than the sum of the true dispersivities:

$$\alpha_{La} + \alpha_{Ta} > \alpha_L + \alpha_T \quad (15)$$

This assumption, that  $\bar{V} = V$ , was included explicitly in Ackerer and Kinzelbach's [1985] apparent dispersivity relations.

In general, the magnitude of the time-averaged velocity is less than the time-averaged magnitude of velocity because the component of velocity that is not oriented in the mean flow direction is not included in the time-averaged velocity. That is,  $|\bar{V}| < |\bar{V}|$ . For the specific case here the magnitude of the time-averaged velocity is smaller than the time-averaged magnitude of velocity by a factor of  $\cos \theta$ . Use of the time-averaged magnitude of velocity will yield a translational (longitudinal) speed of solute movement larger than the actual rate. In practice, the apparent velocity of a plume would be estimated by dividing the distance from the source by the time since solute entered the aquifer. Thus only the longitudinal velocity would contribute to the estimated velocity, consistent with the analysis here.

The ratios of apparent to true dispersivity for longitudinal and transverse components, from (12) and (13) respectively, are functions of  $\theta$  and  $\alpha_T/\alpha_L$ . The apparent longitudinal dispersivity may be larger than the true value if transverse dispersivity is large (Figure 2). Even for large deviation

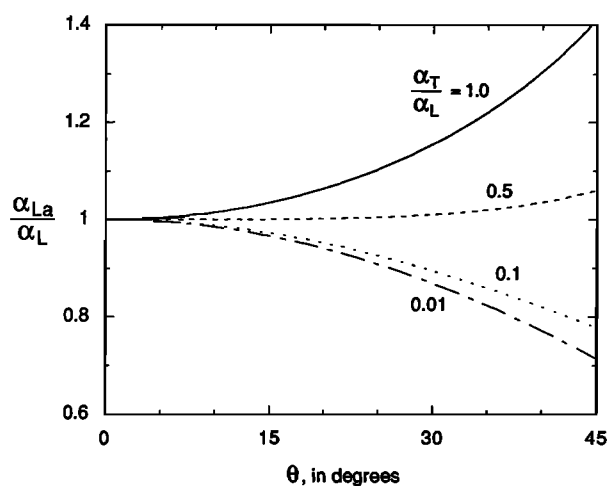


Fig. 2. Ratio of apparent to true longitudinal dispersivity as a function of angle of deviation for several ratios of transverse to longitudinal dispersivity.

angles, the change in longitudinal dispersivity is relatively small. In contrast, the apparent transverse dispersivity can be much larger than the true value, particularly if the transverse dispersivity is small relative to the longitudinal dispersivity (Figure 3).

Under quasi-steady flow conditions, spreading in the direction perpendicular to the mean flow direction is affected by the value of longitudinal dispersivity, as well as by the transverse dispersivity, because the longitudinal component is not always oriented parallel to the mean flow direction. Rather, longitudinal dispersion is oriented in the direction of flow at any instant, and this direction changes over time. The contribution of longitudinal dispersivity to spreading perpendicular to the mean flow direction depends on the angle of deviation between the mean velocity and the velocity at any instant. For this special case of quasi-steady flow, this angle has two values,  $\theta$  and  $-\theta$ . Similarly, solute spreading in the direction of the mean velocity is a function of both longitudinal and transverse dispersivity because the flow vector at any time is not always oriented in its mean direction.

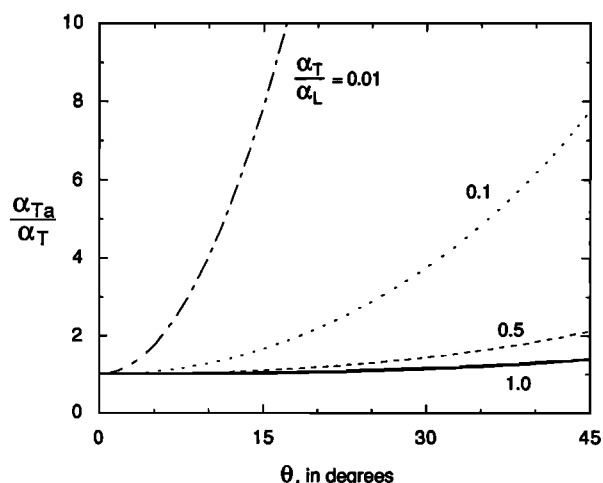


Fig. 3. Ratio of apparent to true transverse dispersivity as a function of angle of deviation for several ratios of transverse to longitudinal dispersivity.

### Examples

Figure 4 shows the potentiometric head for the steady state case, corresponding to the transport problem illustrated in Figure 1 and the first two time periods of a quasi-steady case. The boundary fluxes (per unit width) on the  $y$  boundaries ( $y = \pm 1500$  m) are one half of the fluxes on the  $x$  boundaries ( $Q_y = 0.5 Q_x$ ) and hence  $|V_y| = 0.5 V_x$ . The angle of deviation for this case is, from (8),  $\theta = 26.6^\circ$ . Heads are essentially unchanged along the centerline, but the head contours uniformly rotate in response to changes in the boundary conditions.

Figure 5 shows solute transport in the quasi-steady flow field using the same dispersivities as the steady state flow case shown in Figure 1 ( $\alpha_L = 40$  m;  $\alpha_T = 2$  m). The initial time period is 1 year and, subsequently, the boundary conditions change every 2 years, so that the solute's center of mass returns to the centerline every 2 years (at 2, 4, 6, . . . , 16 years). Figure 5a shows the solute distribution at 4, 8, and 16 years. For comparison, Figure 5b shows the concentration at three selected times (3, 9, and 15 years) when boundary conditions are reversed; during years 3 and 15 the  $y$  velocity was negative, while during year 9 the  $y$  velocity was positive. Spreading in the  $y$  direction in this case is much greater than that shown in Figure 1 for steady state flow. The longitudinal dispersivity acts in the direction of flow which, in this case, is not constantly in the  $x$  direction, as in the steady state case, but varies in time. Although the average or mean flow is in the  $x$  direction, the transient deviations from the mean direction of flow significantly increase spreading in the  $y$  direction. The spatial variance of these plumes is evaluated below in comparison to transient flow results.

Using (12) and (13), the calculated apparent dispersivities for the case shown in Figure 5 are  $\alpha_{La} = 36$  m and  $\alpha_{Ta} = 10.7$  m, and their sum is larger than the sum of the true dispersivities (42 m). Although  $\alpha_{La}$  differs from  $\alpha_L$  by only 10%,  $\alpha_{Ta}$  is more than five times  $\alpha_T$ . Figure 6 shows the analytical solution (10) for a Dirac pulse in quasi-steady flow and the parameters corresponding to the case in Figure 5 at 4 years ( $t_1 = 2$  years) and at 16 years ( $t_1 = 8$  years). Also shown in Figure 6 are the corresponding numerical solutions for the quasi-steady case (from Figure 5a) and for a steady state case using the apparent dispersivity values computed using (12) and (13). The initial conditions are different for the analytical and numerical models (infinitely small point versus four finite difference blocks, an area 200 m by 200 m), although this difference becomes less important as the slug disperses. The small differences between the analytical solution and the numerical solutions are attributed to the different initial conditions and minor numerical dispersion and illustrate the high accuracy of the numerical methods used. The differences between the two numerical solutions are negligible. The solute distribution in a quasi-steady flow field can be accurately matched using steady state flow and apparent dispersivities given by (12) and (13) for those times when the center of mass of solute coincides with the centerline of the assumed steady state flow field (for example, the times shown in Figure 5a). At other times (such as those shown in Figure 5b), the solute distribution cannot be reproduced using a steady state flow field.

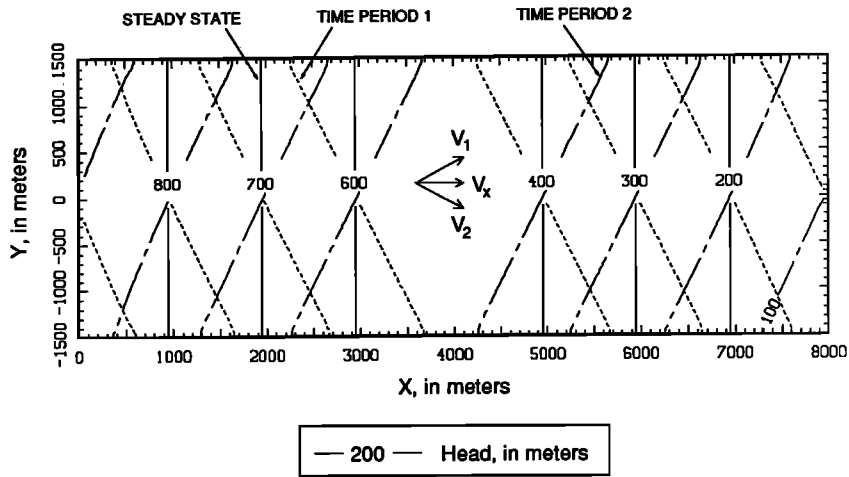


Fig. 4. Head contours for the steady state flow field and the first two time periods for the quasi-steady case having  $|V_y| = 0.5 V_x$ . The velocity vectors during the first ( $V_1$ ) and second ( $V_2$ ) time periods, as well as the constant component of velocity in the  $x$  direction ( $V_x$ ), are illustrated schematically (not to scale).

EFFECTS OF TRANSIENT HYDRAULIC RESPONSE

Characteristic Hydraulic Response Time

The extent to which changes in hydraulic boundary conditions influence solute transport depends, in part, on the

rate at which the aquifer responds to hydraulic stresses. With nonzero storativity the flow system considered here can be modeled as the superposition of one-dimensional steady flow in the  $x$  direction combined with one-dimensional transient flow in the  $y$  direction. From a one-

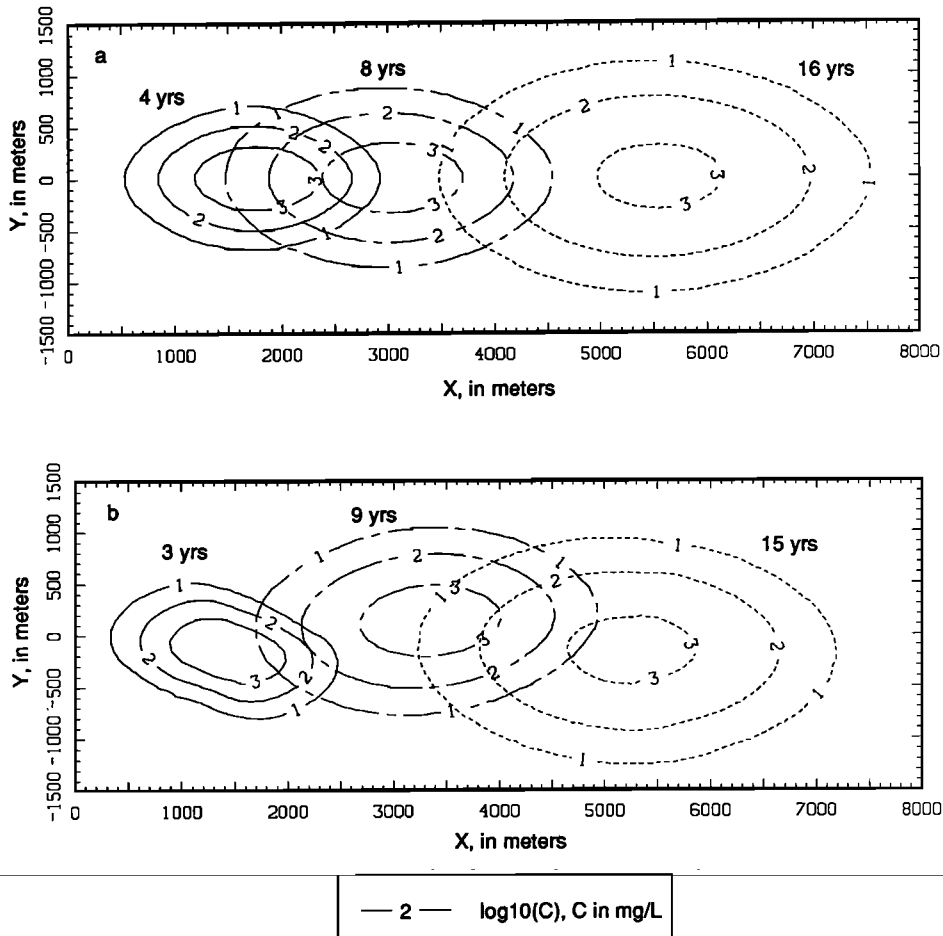


Fig. 5. Solute dispersion in a fluctuating flow field under quasi-steady conditions for  $\alpha_L = 40$  m and  $\alpha_T = 2$  m at (a) 4, 8, and 16 years and (b) 3, 9, and 15 years.

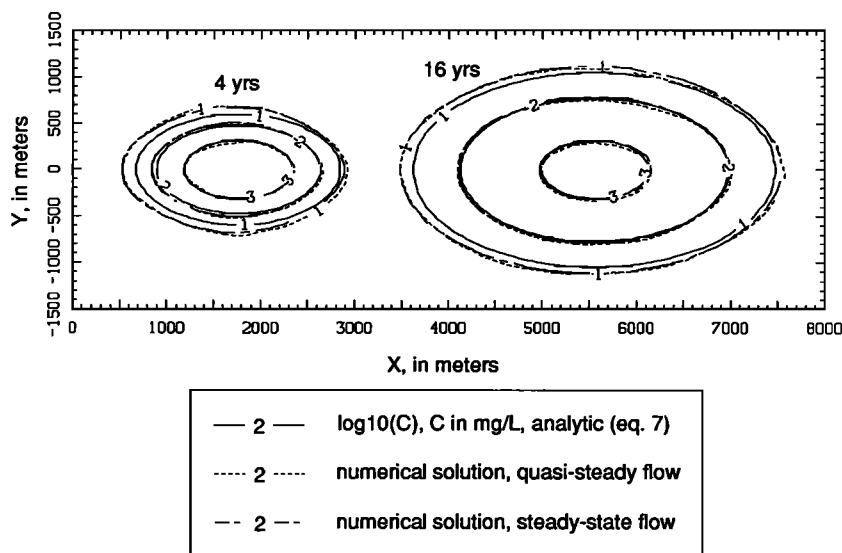


Fig. 6. Solute dispersion in a fluctuating flow field under quasi-steady conditions computed from analytical solution (solid curve) for  $\theta = 26.6$  degrees,  $\alpha_L = 40$  m, and  $\alpha_T = 2$  m. Numerical solution for quasi-steady conditions (dashed curve) from Figure 5a and numerical solution for steady state flow for  $\alpha_{La} = 36$  m and  $\alpha_{Ta} = 10.7$  m (chain-dashed curve) also shown.

dimensional transient flow solution using a specified-head boundary condition and a semi-infinite domain, such as presented by *de Marsily* [1986, p. 198], a characteristic response time  $\tau$  [T] can be derived as

$$\tau = Sy_b^2/4T \tag{16}$$

where  $y_b$  is the distance from the centerline to the top and bottom boundaries [L]. The characteristic response time is inversely proportional to the hydraulic diffusivity ( $T/S$ ). The larger this response time, the slower will be the change in velocities at the model centerline in response to changing boundary conditions. The rate at which the aquifer approaches a new steady state is independent of the magnitude of the boundary condition change. Because this single factor controls transient hydraulic response for this problem, variation of any one of the parameters affecting  $\tau$  can be used to characterize system sensitivity to  $y_b$ ,  $T$ , and  $S$ . For the numerical examples below, storativity ( $S$ ) is changed to show the sensitivity of dispersivity relations to aquifer properties ( $T$  and  $S$ ) and model geometry.

*Examples*

The effects of the aquifer's transient hydraulic response can be examined by comparing solute transport in transient flow to the base case of steady state flow and to quasi-steady flow results. Symmetric stresses result in a transient flow field having the same mean velocity as the base case steady state flow field. The spread of an initially small slug of solute mass, as opposed to a constant source, allows use of the method of moments to quantify dispersion [e.g., *Freyberg*, 1986; *Garabedian et al.*, 1987]. For Fickian dispersion the dispersion coefficient is proportional to the growth in time of the spatial variance of the concentration distribution. The apparent longitudinal dispersion coefficient is proportional to the slope of the  $x$  variance (if flow is assumed to be in the  $x$  direction) of the solute distribution with respect to time. Likewise, the apparent transverse dispersion coefficient is

proportional to the slope of the  $y$  variance with respect to time.

Figure 7 shows the potentiometric head at several times during the first two time periods for a case using the boundary conditions corresponding to the case in Figure 4 ( $Q_y = 0.5 Q_x$ ) but assuming an aquifer storativity of  $S = 0.03$ . The boundary conditions are changed every 2 years, after an initial time period of one year. After each change in boundary conditions the flow equation is solved using an initial time step size of  $5 \times 10^5$  s (about 5.8 days). The time step size is multiplied by 1.4 for each subsequent step, until boundary conditions change again. Time intervals for the solute transport simulation are automatically determined by the model using appropriate stability criteria [*Konikow and Bredehoeft*, 1978] and also limit particle movement each time interval to 0.3 times the grid block dimensions. These time-stepping parameters provide sufficient numerical accuracy for the example flow and transport simulations. Although the head at the centerline does not change significantly, the potentiometric gradient in the  $y$  direction does change, and hence the  $y$  velocity changes. The change in fluid storage in the aquifer causes the changes in velocity in the area of solute mass to lag behind the changes in velocity at the boundaries.

Assuming an aquifer storativity of  $S = 0.03$  (Figure 8) results in less apparent transverse dispersion than the quasi-steady case (see Figure 5a). Because of the time required for the boundary condition changes to propagate into the aquifer, the flow direction near the centerline changes less quickly during a time period for this case than for the quasi-steady ( $S = 0$ ) case. The flow directions near the centerline of the flow field shown in Figure 7 rotate through a range of directions within an arc of about  $53^\circ$ . However, under transient flow conditions the actual flow direction is at the extremes of this range for much shorter times than under quasi-steady flow conditions. For greater characteristic response time and shorter time periods, flow direction changes at the centerline may be negligible. Also, the solute's center

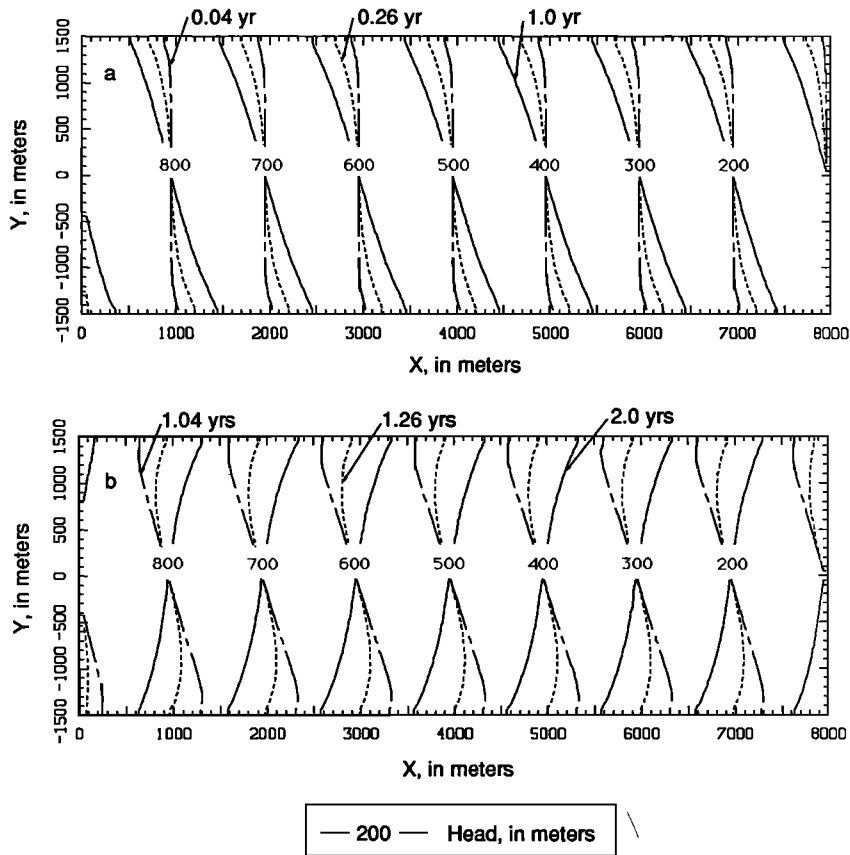


Fig. 7. Head contours for transient flow field ( $S = 0.03$ ) having  $Q_y = 0.5 Q_x$  at several times during the (a) first and (b) second time periods.

of mass does not return exactly to the centerline every 2 years as in the quasi-steady case because of the imposed initial condition of uniform flow in the  $x$  direction. For the quasi-steady case, flow is at an angle  $\theta$  instantly at  $t = 0$ .

Figures 9 and 10 show the growth in time of  $x$  and  $y$  variance, respectively, for the steady state and quasi-steady cases, corresponding to Figures 1 and 5, respectively, and for transient cases assuming  $S = 0.1$ ,  $S = 0.03$  (corresponding to Figure 8), and  $S = 0.01$ . Slight decreases in the slope of the  $x$  variance are shown, but the differences are relatively

insignificant. However, Figure 10 shows significant changes in solute spreading in the  $y$  direction, depending on the value of storativity or the corresponding value of characteristic response time. If the storativity is 0.1, the solute spreading in the  $y$  direction is only slightly increased by the boundary condition transients compared to the steady state flow condition. When the storativity equals 0.01, transverse spreading is increased almost as much as in the quasi-steady case ( $S = 0$ ). Varying storativity (and hence proportionally varying characteristic response time), the effects of boundary

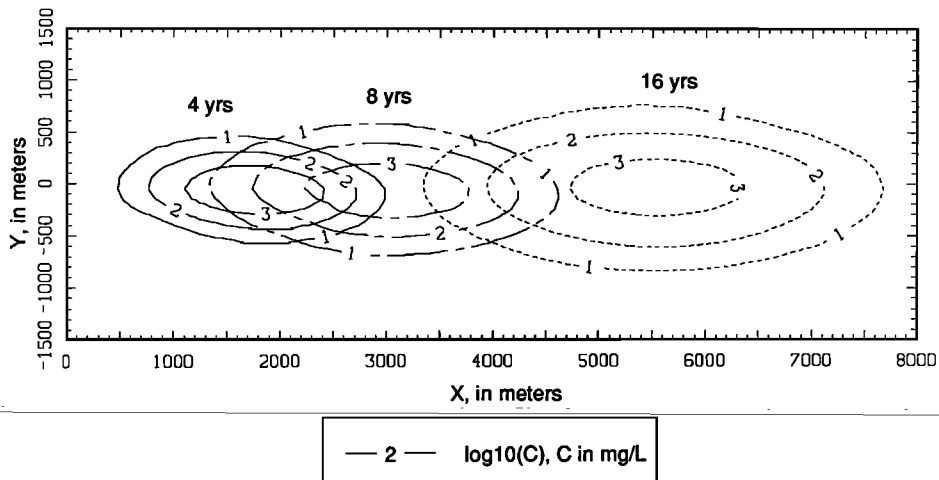


Fig. 8. Solute dispersion in fluctuating flow field under transient conditions ( $S = 0.03$  and  $Q_y = 0.5 Q_x$ ) for  $\alpha_L = 40$  m and  $\alpha_T = 2$  m.

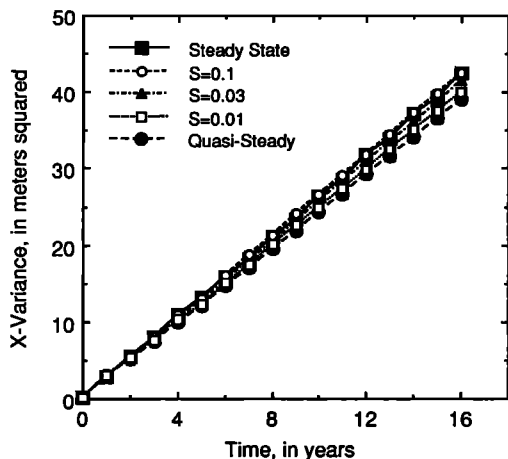


Fig. 9. Concentration variance in the  $x$  direction (longitudinal) as a function of time for steady state flow, transient flow, and quasi-steady flow for  $Q_y = 0.5 Q_x$ ,  $\alpha_L = 40$  m, and  $\alpha_T = 2$  m.

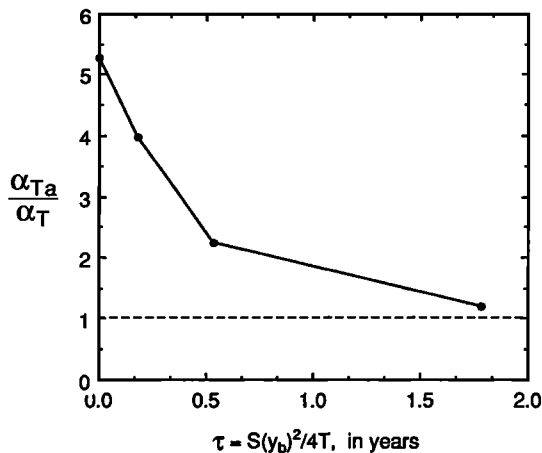


Fig. 11. Ratio of apparent to true transverse dispersivity as a function of characteristic response time.

condition transients on solute dispersion range from the results shown for the quasi-steady case for small characteristic response time to no effects for large characteristic response time (Figure 11).

On the basis of concentration data alone, an investigator might interpret these patterns of solute spreading (Figures 5 and 8) as resulting from a higher transverse dispersivity caused by aquifer heterogeneity and not expect that they had been caused in part by temporal variations in the flow field. Predictions of a model having uniform steady state flow but using a high transverse dispersivity would be similar to actual transport under transient conditions only as long as the hydraulic transients continue in the same manner. If the transients stop, or if the plume spreads beyond the area influenced by the transients, transverse spreading could be significantly overestimated.

EFFECTS OF FREQUENCY OF VELOCITY CHANGE ON PLUME SHAPE

The shape of a plume from a constant source of solute mass may indicate past flow directions and rates. Figure 12

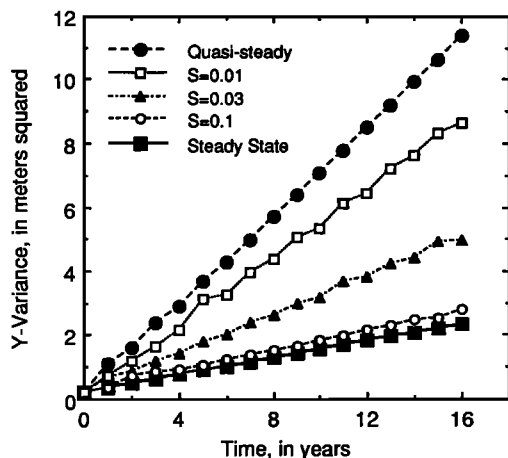


Fig. 10. Concentration variance in  $y$  direction (transverse) as a function of time for steady state flow, transient flow, and quasi-steady flow for  $Q_y = 0.5 Q_x$ ,  $\alpha_L = 40$  m, and  $\alpha_T = 2$  m.

shows a plume at 16 years in a quasi-steady flow field, using the same hydraulic characteristics and dispersivities as the case in Figure 5 but having solute mass added continually at a constant rate and having a longer time between boundary condition changes (4 years). Because the time between boundary condition changes for this case (4 years) is long relative to the travel time of the plume (16 years), the plume shape is distinct from the expected plume shape in a steady state, uniform flow field. Of course, the ability to make this distinction in real plumes would be hindered typically by a lack of data.

When boundary condition changes occur at a high frequency (short time periods) relative to the plume's advection, past hydraulic transients may not be readily apparent from plume shape, even with dense spatial sampling. In aquifers having large storativity a high frequency of boundary condition changes would also reduce the apparent dispersion effect because the boundary stresses would not propagate as far into the aquifer in a shorter time. Figure 13 shows a plume that results from the same source, dispersion, and quasi-steady flow conditions as the case in Figure 12 but having a shorter time period between boundary condition changes (1 year). For this high-frequency case the transient nature of the flow field is not readily apparent in the plume shape because the plume does not have sufficient time to move far from the centerline during each short stress period. In addition, dispersion smooths out small variations in the concentration distribution. The overall width (maximum extent from centerline) of this plume (Figure 13) is slightly less than that in Figure 12. Because typical field investigations are based on a limited number of concentration data, gross plume characteristics, such as maximum width during the sampling period, may be misinterpreted as being indicative of dispersion rather than lateral movement of the plume due to hydraulic transients.

The effects of transient changes in flow are further illustrated by examining concentration changes over time at fixed points in space. Figure 14 shows how concentration would change with time near the flow field centerline ( $x = 1950$  m,  $y = -50$  m) for the cases shown in Figures 12 and 13 and for the case of steady state flow using the apparent dispersivities  $\alpha_{La} = 36$  m, and  $\alpha_{Ta} = 10.7$  m. As expected, the steady state flow case yields a relatively smooth breakthrough curve.

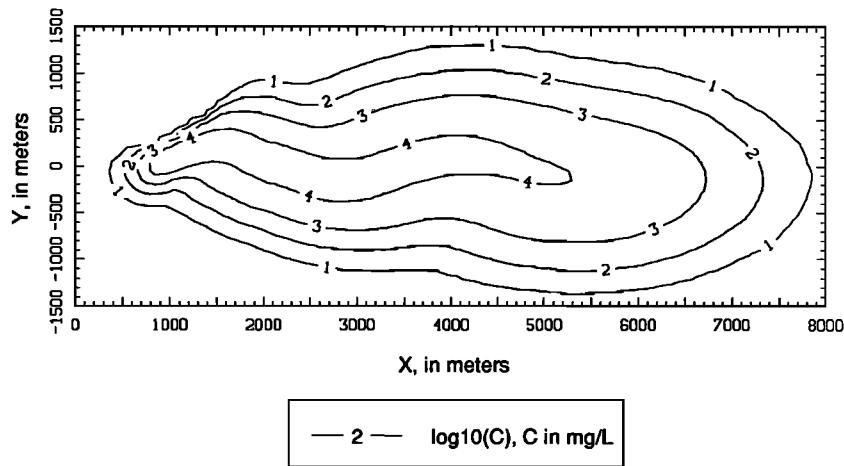


Fig. 12. Plume at 16 years from constant solute source in fluctuating flow field under quasi-steady conditions having 4 years between boundary condition changes and  $\alpha_L = 40$  m and  $\alpha_T = 2$  m.

(The minor oscillations result from the numerical model's procedures in converting concentrations of tracer particles within the area of a finite difference cell to average concentration at the node [see Konikow and Bredehoeft, 1978].) However, significant fluctuations in concentration are indicated for the quasi-steady flow cases, which are indicators of behavior under true transient flow conditions. For the lower frequency of boundary condition changes (4 years between changes, corresponding to the plume shown in Figure 12), the range of fluctuation is almost 100% of the peak concentrations. For the higher frequency of boundary conditions changes (1 year between changes, corresponding to the plume in Figure 13) the range of fluctuation is about 40% of the peak. This very high temporal variability could be encountered in the field and indicates the need for multiple synoptic sampling periods to adequately characterize a plume in a transient flow field.

#### CONCLUSIONS

Theoretical and field analyses indicate that longitudinal dispersivity is scale-dependent in porous media and that transverse dispersivity is generally one or more orders of magnitude smaller [e.g., Dagan, 1982; Gelhar and Axness,

1983], causing solute plumes to be long and thin. However, some observed plumes appear to be relatively wide and apparently have a relatively large transverse dispersivity. As shown here, it is possible that some part of this large transverse dispersivity might be due to transient changes in the flow field that were not recognized and (or) explicitly incorporated into solute transport analyses.

When concentrations are observed in a flow field that previously underwent hydraulic transients, the flow field may have returned to a steady state condition. For the cases examined here, observations of potentiometric head at such a time would show uniform steady flow in the  $x$  direction, and these observations would provide no indication of past transients that controlled fluid path lines. When few or no historic potentiometric head or solute concentration data are available, as is typical of contamination sites, it may be impossible to ascertain the past hydrologic regimes and their effect on observed solute spreading, as shown by these examples.

Unrecognized flow field transients that change the direction of flow of a plume cause an apparent increase in transverse dispersivity because longitudinal dispersion is acting in a direction that is not parallel to the assumed flow

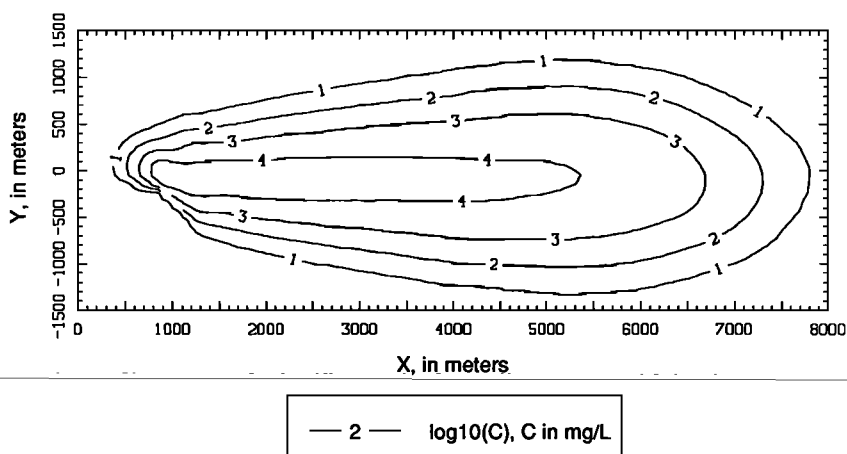


Fig. 13. Plume for same conditions as Figure 12 except time between boundary condition changes is 1 year.

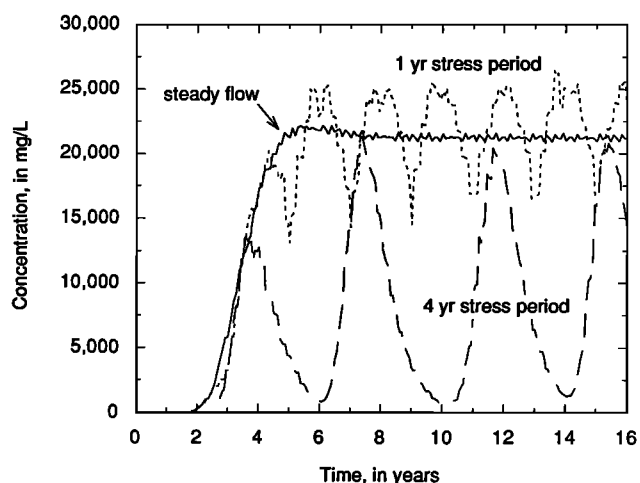


Fig. 14. Concentration as a function of time for an observation point located at  $(x = 1950 \text{ m}, y = -50 \text{ m})$  from constant solute source in steady state flow field for  $\alpha_{La} = 36 \text{ m}$  and  $\alpha_{Ta} = 10.7 \text{ m}$  and in fluctuating flow fields under quasi-steady conditions having 4 years and 1 year between boundary condition changes for  $\alpha_L = 40 \text{ m}$  and  $\alpha_T = 2 \text{ m}$ .

direction. If flow field transients are symmetric in time and space, resultant plumes closely resemble plumes that evolve in uniform, steady state flow fields having the same mean velocity. Having limited spatial data and no historic record of heads and concentrations, it will be difficult to distinguish between the effects of aquifer heterogeneity and hydraulic transients on solute distribution. Asymmetric transients (for example, those caused by pumping or recharge only along one side of the flow field) may significantly increase the spreading of the plume in a direction transverse to the assumed flow direction. Given adequate data, however, the cause of this effect may be discernible from the plume shape and position.

The increase in apparent transverse dispersivity under transient flow primarily is a function of the extent of change in flow direction and the ratio of longitudinal to transverse dispersivity. For the example problem using a 20:1 ratio of longitudinal to transverse dispersivity and a  $26.6^\circ$  angle of deviation of the transient flow vector from the mean, apparent transverse dispersivity increases by a factor of about five. The apparent transverse dispersivity may be larger than the apparent longitudinal dispersivity when flow directions change through a wide angle, even if the true transverse dispersivity is zero. Thus flow field transients that are not recognized or accounted for in transport simulations may result in significant overestimates of transverse dispersivity during model calibration. Subsequent changes in the nature of the hydraulic transients will significantly diminish the predictive accuracy of simulations using a transverse dispersivity that was calibrated to an erroneously high value.

The magnitude of the effect of changes in hydraulic boundary conditions or stresses on apparent dispersivity is inversely related to the system's characteristic response time. Thus the maximum effect on apparent dispersivity occurs under quasi-steady flow conditions. For transient flow systems ( $S \neq 0$ ) the magnitude of the effect is reduced, depending on the hydraulic diffusivity of the aquifer and the geometric properties of the system, as expressed in the system's characteristic response time (equation (16)). The

effect is greater for higher transmissivity and it decreases with increasing storativity and distance to aquifer boundaries. Boundary condition transients are important when they occur over a time period long enough relative to the system's characteristic response time for a change in flow direction to propagate to the location of solute mass.

Apparent dispersivities change because of the ignored or unknown change in flow direction and because the apparent velocity magnitude is smaller than the true velocity magnitude. The relations between apparent and true dispersivities are derived using an analytical solution for transport in a fluctuating, quasi-steady flow field, and they depend on the angle of deviation of the velocity vector from the mean and the ratio of transverse to longitudinal dispersivity (equations (12) and (13)). These apparent dispersivities are similar to those presented by *Kinzelbach and Ackerer* [1986], but here we clarify the effect of the difference between the apparent or time-averaged velocity and the true velocity magnitude. The apparent longitudinal dispersivity can be larger or smaller than the true longitudinal dispersivity, depending on the ratio of transverse to longitudinal dispersivity. Either way, the effects on longitudinal spreading are generally much smaller than the effects on transverse spreading. These results are qualitatively similar to those of *Rehfeldt* [1988], based on stochastic theory. The apparent transverse dispersivity can be many times larger than the true transverse dispersivity when the ratio of transverse to longitudinal dispersivity is small. In this case, even relatively small deviations in the direction of flow ( $10^\circ$  angle of deviation from the mean) can significantly increase transverse spreading.

#### APPENDIX: ANALYTICAL SOLUTION FOR SOLUTE DISPERSION IN A FLUCTUATING, QUASI-STEADY, UNIFORM FLOW FIELD

Convolution can be used to obtain an analytical solution for solute dispersion in a fluctuating, uniform flow field under quasi-steady conditions. An initial point source of solute mass is released at the origin ( $x = 0, y = 0$ ). Flow is initially at an angle  $\theta$  to the  $x$  axis. After some time  $t_1$ , the flow field changes direction instantly to  $-\theta$ . The solute distribution during the second time period is the convolution of the distribution at the end of the first period (the initial condition for the second period) times the solution (Green's function) for an instantaneous point source.

The analytical solution for the spread of a solute in uniform flow (in the  $x$  direction) in an infinite plane from an instantaneous injection of a unit mass at the origin is [after *Bear*, 1979]

$$C(x, y, t) = \frac{1}{\epsilon b} (4\pi Vt)^{-1} (\alpha_L \alpha_T)^{-1/2} \cdot \exp \left[ -\frac{(x - Vt)^2}{4\alpha_L Vt} - \frac{y^2}{4\alpha_T Vt} \right] \quad (\text{A1})$$

If the flow vector is at an angle  $\theta$  to the  $x$  axis and the injection occurs at  $X, Y$ , the solution is

$$C(x, y, t) = \frac{1}{\epsilon b} (4\pi Vt)^{-1} (\alpha_L \alpha_T)^{-1/2} \cdot \exp \left\{ - \frac{[(x - X) \cos \theta + (y - Y) \sin \theta - Vt]^2}{4\alpha_L Vt} - \frac{[(y - Y) \cos \theta - (x - X) \sin \theta]^2}{4\alpha_T Vt} \right\} \quad (A2)$$

Because the governing equation is linear, the concentration distribution from an arbitrary initial condition is the convolution of the initial condition and the solution for an instantaneous point injection:

$$C(x, y, t) = \frac{1}{\epsilon b} \int_{-\infty}^{\infty} \int_{-\infty}^{\infty} \epsilon b C_I(X, Y, t_1) \cdot \epsilon b C(x - X, y - Y, t - t_1) dX dY \quad (A3)$$

where  $C_I(X, Y, t_1)$  is the initial condition for the second time period beginning at time  $t = t_1$ . During this first time period,  $0 < t < t_1$ , the flow direction is at angle  $\theta$  to the  $x$  axis. At time  $t_1$  the flow direction switches instantly to an angle  $-\theta$ . Using (A2) for the initial condition,  $C_I$  at time  $t_1$ , and using (A2) and an angle of  $-\theta$  for the instantaneous solution at time  $t > t_1$ , the convolution (A3) is

$$C(x, y, t) = \frac{1}{\epsilon b} \int_{-\infty}^{\infty} \int_{-\infty}^{\infty} (4\pi Vt_1)^{-1} (\alpha_L \alpha_T)^{-1/2} \cdot \exp \left\{ - \frac{[X \cos \theta + Y \sin \theta - Vt_1]^2}{4\alpha_L Vt_1} - \frac{[Y \cos \theta - X \sin \theta]^2}{4\alpha_T Vt_1} \right. \\ \cdot [4\pi V(t - t_1)]^{-1} (\alpha_L \alpha_T)^{-1/2} \cdot \exp \left\{ - \frac{[(x - X) \cos \theta - (y - Y) \sin \theta - V(t - t_1)]^2}{4\alpha_L V(t - t_1)} - \frac{[(y - Y) \cos \theta + (x - X) \sin \theta]^2}{4\alpha_T V(t - t_1)} \right\} dX dY \quad (A4)$$

where we have used  $\cos(-\theta) = \cos(\theta)$  and  $\sin(-\theta) = -\sin(\theta)$ .

Equation (A4) may be integrated for the general case using equation 3.323 from *Gradshteyn and Ryzhik* [1980]:

$$C(x, y, t) = \frac{1}{\epsilon b} (4V)^{-2} [\pi \alpha_L \alpha_T t_1(t - t_1)]^{-1} (P_x P_y)^{-1} \cdot \exp \left\{ - \frac{[x \cos \theta - y \sin \theta - V(t - t_1)]^2}{4\alpha_L V(t - t_1)} - \frac{(x \sin \theta + y \cos \theta)^2}{4\alpha_T V(t - t_1)} - \frac{(Vt_1)^2}{4\alpha_L Vt_1} + \frac{\cos^2 \theta (Vt_1)^2}{(4\alpha_L Vt_1)^2 P_x^2} \right. \\ \left. + \frac{\cos^2 \theta [x \cos \theta - y \sin \theta - V(t - t_1)]^2}{[4\alpha_L V(t - t_1)]^2 P_x^2} \right.$$

$$+ \frac{2 \cos^2 \theta Vt_1 [x \cos \theta - y \sin \theta - V(t - t_1)]}{[4\alpha_L Vt_1][4\alpha_L V(t - t_1)] P_x^2} + \frac{\sin^2 \theta (x \sin \theta + y \cos \theta)^2}{[4\alpha_T V(t - t_1)]^2 P_x^2} + \frac{2 \sin \theta \cos \theta Vt_1 (x \sin \theta + y \cos \theta)}{[4\alpha_L Vt_1][4\alpha_T V(t - t_1)] P_x^2} + \frac{2 \sin \theta \cos \theta [x \cos \theta - y \sin \theta - V(t - t_1)] [x \sin \theta + y \cos \theta]}{[4\alpha_L V(t - t_1)][4\alpha_T V(t - t_1)] P_x^2} + \left. \frac{Z^2}{4P_y^2} \right\} \quad (A5)$$

where

$$P_x^2 = \frac{\cos^2 \theta}{4\alpha_L Vt_1} + \frac{\sin^2 \theta}{4\alpha_T Vt_1} + \frac{\cos^2 \theta}{4\alpha_L V(t - t_1)} + \frac{\sin^2 \theta}{4\alpha_T V(t - t_1)} \quad (A6)$$

$$P_y^2 = \frac{\cos^2 \theta}{4\alpha_T Vt_1} + \frac{\sin^2 \theta}{4\alpha_L Vt_1} + \frac{\cos^2 \theta}{4\alpha_T V(t - t_1)} + \frac{\sin^2 \theta}{4\alpha_L V(t - t_1)} + \frac{\sin^2 \theta \cos^2 \theta}{P_x^2} \{ - (4\alpha_L Vt_1)^{-2} - (4\alpha_T Vt_1)^{-2} + 2(4\alpha_L Vt_1)^{-1} (4\alpha_T Vt_1)^{-1} - [4\alpha_L V(t - t_1)]^{-2} + 2(4\alpha_L Vt_1)^{-1} [4\alpha_L V(t - t_1)]^{-1} - [4\alpha_T V(t - t_1)]^{-2} - 4(4\alpha_L Vt_1)^{-1} [4\alpha_T V(t - t_1)]^{-1} + 2(4\alpha_T Vt_1)^{-1} [4\alpha_T V(t - t_1)]^{-1} + 2[4\alpha_L V(t - t_1)]^{-1} [4\alpha_T V(t - t_1)]^{-1} \} \quad (A7)$$

$$Z = \frac{2 \sin \theta Vt_1}{4\alpha_L Vt_1} + \frac{2y \sin^2 \theta - 2x \sin \theta \cos \theta + 2 \sin \theta V(t - t_1)}{4\alpha_L V(t - t_1)} + \frac{2y \cos^2 \theta + 2x \sin \theta \cos \theta}{4\alpha_T V(t - t_1)} + \frac{2 \sin \theta \cos \theta}{P_x^2} \left\{ - \frac{\cos \theta Vt_1}{(4\alpha_L Vt_1)^2} + \frac{\cos \theta Vt_1}{(4\alpha_L Vt_1)(4\alpha_T Vt_1)} \right. \\ \left. + \frac{\cos \theta Vt_1 - x \cos^2 \theta + y \sin \theta \cos \theta + \cos \theta V(t - t_1)}{[4\alpha_L Vt_1][4\alpha_L V(t - t_1)]} + \frac{x \cos^2 \theta - y \sin \theta \cos \theta - \cos \theta V(t - t_1)}{[4\alpha_L V(t - t_1)]^2} + \frac{x \cos^2 \theta - y \sin \theta \cos \theta - \cos \theta V(t - t_1)}{[4\alpha_T Vt_1][4\alpha_L V(t - t_1)]} \right. \\ \left. - \frac{x \sin^2 \theta - y \sin \theta \cos \theta - \cos \theta Vt_1}{[4\alpha_L Vt_1][4\alpha_T V(t - t_1)]} + \frac{x \sin^2 \theta + y \sin \theta \cos \theta}{[4\alpha_T Vt_1][4\alpha_T V(t - t_1)]} \right.$$

$$\begin{aligned}
 & + \frac{x \sin^2 \theta - x \cos^2 \theta + 2y \sin \theta \cos \theta + \cos \theta V(t - t_1)}{[4\alpha_L V(t - t_1)][4\alpha_T V(t - t_1)]} \\
 & + \frac{-x \sin^2 \theta - y \sin \theta \cos \theta}{[4\alpha_T V(t - t_1)]^2} \} \quad (A8)
 \end{aligned}$$

It is possible to perform this convolution (and integration) for multiple time periods of arbitrary length. The analytical results presented in Figure 6 are computed using a numerical implementation of (A5)–(A8).

This analytical solution may be useful for testing grid orientation effects in numerical solutions of the transport equation. The orientations of longitudinal and transverse dispersion components change from the first time period to the second. During the second time period the long axis of the plume changes orientation as time increases. Because the flow direction changes, it is not possible to orient the numerical grid with the flow direction for both the first and second time periods.

When the second time period equals the first time period ( $t = 2t_1$ ;  $t - t_1 = t_1$ ), the center of the plume has returned to the  $x$  axis, and (A5) reduces to

$$\begin{aligned}
 C(x, y, t) = & \frac{1}{\epsilon b} (4\pi Vt)^{-1} [(\alpha_L \cos^2 \theta + \alpha_T \sin^2 \theta) \\
 & \cdot (\alpha_T \cos^2 \theta + \alpha_L \sin^2 \theta)]^{-1/2} \\
 & \cdot \exp \left[ -\frac{(x - Vt \cos \theta)^2}{4(\alpha_L \cos^2 \theta + \alpha_T \sin^2 \theta)Vt} \right. \\
 & \left. - \frac{y^2}{4(\alpha_T \cos^2 \theta + \alpha_L \sin^2 \theta)Vt} \right] \quad (A9)
 \end{aligned}$$

which can be written

$$\begin{aligned}
 C(x, y, t) = & \frac{1}{\epsilon b} (4\pi V_a t)^{-1} (\alpha_{La} \alpha_{Ta})^{-1/2} \\
 & \cdot \exp \left[ -\frac{(x - V_a t)^2}{4\alpha_{La} V_a t} - \frac{y^2}{4\alpha_{Ta} V_a t} \right] \quad (A10)
 \end{aligned}$$

where

$$V_a = V \cos \theta \quad (A11)$$

$$\alpha_{La} = \alpha_L \cos \theta + \alpha_T \sin \theta \tan \theta \quad (A12)$$

$$\alpha_{Ta} = \alpha_T \cos \theta + \alpha_L \sin \theta \tan \theta \quad (A13)$$

This form is directly analogous to the solution for dispersion in a uniform steady state flow field (A1). As long as the time periods have the same length, and the angle of flow is the same ( $\theta$  or  $-\theta$ ), the relations in (A11)–(A13) are valid, and (A10) is the solute distribution at  $t = 2t_1, 4t_1, 6t_1, \dots, (2n)t_1$ . For cases of  $\alpha_L$  greater than  $\alpha_T$ , and  $\theta$  less than  $90^\circ$ , this plume is oriented with its long axis in the direction of the mean velocity. At other times ( $t \neq (2n)t_1$ ) the plume's long axis will not be aligned in the mean flow direction.

*Acknowledgment.* We are grateful to Allen M. Shapiro, U.S. Geological Survey, for assistance to us on the mathematics in the appendix and for suggestions on the manuscript.

REFERENCES

Ackerer, P., and W. Kinzelbach, Modelisation du transport de contaminant par la methode de marche au hasard—Influence des variations du champ d'ecoulement au cours du temps sur la dispersion, paper presented at the Symposium on the Stochastic Approach to Subsurface Flow, Int. Assoc. of Hydraul. Res., Montvillargenne, France, June 3–6, 1985.

Bear, J., *Hydraulics of Groundwater*, 567 pp., McGraw-Hill, New York, 1979.

Dagan, G., Stochastic modeling of groundwater flow by unconditional and conditional probabilities, 2, The solute transport, *Water Resour. Res.*, 18(4), 835–848, 1982.

Dagan, G., Solute transport in heterogeneous porous media, *J. Fluid Mech.*, 145, 151–177, 1984.

de Marsily, G., *Quantitative Hydrogeology*, 440 pp., Academic, San Diego, Calif., 1986.

Duguid, J. O., and M. Reeves, A comparison of mass transport using average and transient rainfall boundary conditions, in *Finite Elements in Water Resources Proceedings of the First International Conference on Finite Elements in Water Resources, July 1976, Princeton, N. J.*, edited by W. G. Gray, G. F. Pinder, and C. A. Brebbia, pp. 2.25–2.35, Pentech, London, 1977.

Freyberg, D. L., A natural gradient experiment on solute transport in a sand aquifer, 2, Spatial moments and the advection and dispersion of nonreactive tracers, *Water Resour. Res.*, 22(13), 2031–2046, 1986.

Garabedian, S. P., D. R. LeBlanc, K. M. Hess, and R. D. Quadri, Natural-gradient tracer test in sand and gravel—Results of spatial moments analysis, U.S. Geological Survey Program on Toxic Waste—Ground-Water Contamination, Proceedings of the Third Technical Meeting, Pensacola, Florida, March 23–27, 1987, edited by B. J. Franks, *U.S. Geol. Surv. Open File Rep. 87-109*, B13–B16, 1987.

Gelhar, L. W., and C. L. Axness, Three-dimensional stochastic analysis of macrodispersion in aquifers, *Water Resour. Res.*, 19(1), 161–180, 1983.

Goode, D. J., and L. F. Konikow, Modification of a method-of-characteristics solute-transport model to incorporate decay and equilibrium-controlled sorption or ion exchange, 65 pp., *U.S. Geol. Surv. Water Resour. Invest. Rep. 89-4030*, 1989.

Gradshteyn, I. S., and I. M. Ryzhik, *Table of Integrals, Series, and Products*, 1160 pp., Academic, San Diego, Calif., 1980.

Kinzelbach, W., and P. Ackerer, Modelisation de la propagation d'un contaminant dans un champ d'ecoulement transitoire, *Hydrogeologie*, 2, 197–205, 1986.

Konikow, L. F., and J. D. Bredehoeft, Computer model of two-dimensional solute transport and dispersion in ground water, *U.S. Geol. Surv. Tech. Water Resour. Invest.*, 7-C2, 90 pp., 1978.

Konikow, L. F., and D. B. Grove, Derivation of equations describing solute transport in ground water, 30 pp., *U. S. Geol. Surv. Water Resour. Invest. Rep. 77-19*, 1977.

LaFave, J. I., The effect of an intermittent stream on a shallow groundwater system and the implications for groundwater remediation, in *Proceedings of the Third National Outdoor Action Conference*, pp. 719–732, National Water Well Association, Dublin, Ohio, 1989.

Naff, R. L., T.-C. J. Yeh, and M. W. Kemblowski, Reply, *Water Resour. Res.*, 25(12), 2523–2525, 1989.

Rehfeldt, K. R., Prediction of macrodispersivity in heterogeneous aquifers, 233 pp., Ph.D. thesis, Dep. of Civil Eng., Mass. Inst. of Technol., Cambridge, 1988.

Sykes, J. F., S. B. Pahwa, R. B. Lantz, and D. S. Ward, Numerical simulation of flow and contaminant migration at an extensively monitored landfill, *Water Resour. Res.*, 18(6), 1687–1704, 1982.

Wierenga, P. J., Solute distribution profiles computed with steady-state and transient water movement models, *Soil Sci. Soc. Am. J.*, 41, 1050–1055, 1977.

D. J. Goode and L. F. Konikow, U.S. Geological Survey, 431 National Center, Reston, VA 22092.

(Received September 21, 1989;  
revised March 21, 1990;  
accepted June 13, 1990.)